Presented at the Topical Conference on
Neutrino Physics at Accelerators,
Oxford, England, July 3-7, 1978

LBL-7908

PERFORMANCE CHARACTERISTICS OF THE FERMILAB 15-FOOT BUBBLE CHAMBER WITH A 1/3-SCALE INTERNAL PICKET FENCE (IPF) AND A TWO-PLANE EXTERNAL MUON IDENTIFIER (EMI)

M. L. Stevenson

June 1978

Prepared for the U. S. Department of Energy
under Contract W-7405-ENG-48

MASTER

LBL-7908

Submitted to the Topical Conference
on Neutrino Physics at Accelerators,
Oxford, England July 3-7, 1978, by
M. L. Stevenson

PERFORMANCE CHARACTERISTICS OF THE FERMILAB 15-FOOT BUBBLE CHAMBER WITH A 1/3-SCALE INTERNAL PICKET FENCE (IPF) AND A TWO-PLANE EXTERNAL MUON IDENTIFIER (EMI)*

Berkeley (LBL)†, Fermilab, Hawaii, Seattle,
Wisconsin Collaboration[1)]

NOTICE

*This work was supported primarily by the High Energy Physics Division of the Department of Energy.

†Lawrence Berkeley Laboratory, Berkeley, California

ABSTRACT

The Fermilab 15-foot bubble chamber has been exposed to a quadrupole triplet neutrino beam. During this exposure, a 2-plane EMI and a 1/3-scale IPF, were in operation downstream of the bubble chamber. The IPF consisted of sixteen 0.1 m^2 drift chambers (pickets) placed inside the vacuum tank of the bubble chamber to record temporal information from neutrino interactions. When a $\geqslant$5-fold time coincidence between one or more of the pickets of the IPF and the EMI was formed, one was able to search the magnetic tapes for dimuon candidates. Even with 1/3 geometrical coverage by the IPF, this system identified 70% of the dimuon candidates before the film was scanned. Other performance characteristics of the system will be presented with emphasis on the usefulness of the IPF.

CONTENTS

	Page
I. INTRODUCTION	1
II. 15-FOOT BUBBLE CHAMBER MOMENTUM (CURVATURE) ACCURACY	2
III. EMI AS CONFIGURED FOR E-546	3
III.1. Geometrical Efficiency	3
III.2. Muon Identification Efficiency	3
III.2.1. Electronic efficiency from beam tracks	3
III.2.2. Electronic efficiency from muons from ν interaction	5
III.2.3. In-time background	5
IV. THE INTERNAL PICKET FENCE	6
IV.1. Geometrical Efficiency	6
IV.1.1. E-546 Arrangement as a 1/3-scale model	6
IV.1.2. New Configuration and improvements	7
IV.2. Electronic Efficiency	7
IV.3. IPF "triggering" Efficiency	8
IV.3.1. Charged current events of E-546	8
IV.3.2. Dimuon events of E-546 ("GSCAN") candidates)	9
IV.3.3. Neutral current (NC) events of E-546	11
IV.3.4. Predicted performance for NC identification for dichromatic experiments E-380/388.	12
V. SUMMARY	13
V.1. The Curvature ($K \equiv p^{-1}$) Accuracy of the 15-Foot Bubble Chamber is, $\Delta K \approx 3/\ell^2(m)$ Tev^{-1}.	13
V.2. The Geometrical Efficiency of the 2-plane EMI for CC($\overline{CC}$) Events of E-546 is 0.85±.03 (0.91±.03)	13

CONTENTS (Cont'd)

Page

V.3. The Electronic Efficiency of the 1st (2nd) Plane is .94±.01 (.92±.01) 13

V.4.1. The geometrical efficiency of the IPF for E-546 is 0.30. For the improved IPF it will be nearly 1 13

V.4.2. The electronic efficiency of the average picket is 0.77. 13

V.4.3.1. The efficiency for the IPF to "fire" on an E-546 CC event is 0.66 13

V.4.3.2. The efficiency for the IPF to "find" dimuon events from the EMI tapes is 0.66±.11 13

V.4.3.3. The efficiency for the IPF to "fire" on an E-546 NC event is ≈0.61. The geometrical efficiency of the 2-plane EMI for positive (negative) hadrons (P>4GeV/c) from CC events is 0.94(0.82) 13

V.4.3.4. The efficiency for the improved IPF to "fire" on a NC event of E 380/388 will be nearly 1. It is too early for us to predict what the geometrical efficiency of the EMI will be for hadrons. 13

VI. ACKNOWLEDGEMENTS 14

REFERENCES 15

FIGURES 16

I. INTRODUCTION

For most of the experiments performed in the Fermilab 15-foot bubble chamber, the EMI has suffered from a large random background of particles that traverse its one plane. This background, which amounts to 5 to 10 per m^2 per 10^{13} protons/pulse depending on the focussing system, causes problems in identifying slow muons. The typical multiple scattering of muons in traversing the 3 to 5 pion absorpton length thick absorber in front of the EMI is such that 86% of them lie within a circle of radius, 22 cm/p (GeV/c). For a 5 GeV/c particle, this amounts to a 10% probability of misidentification. Often these muons are the most interesting ones, coming from "high-y" neutrino interactions which are most likely to reveal new physics phenomena.

By adding a second EMI plane as well as an IPF, it is possible to eliminate this random background by determing when during the beam spill the charged current (CC) or (NC) interaction occurred.

One of the physics objectives of experiment E-546 was to observe the hadronic state of dilepton events at higher energies than before. It was our belief that the most bias-free way was to observe dimuons events rather than μ-e events and to fill the bubble chamber with a lighter mix of Ne. It becomes increasingly difficult to observe electrons or positrons emerging from a vertex that is more tightly collimated and contains more tracks. We

chose a 47% Ne-H mixture which has a radiation length of 54 cm and an interaction length of 1.9 m.

Section II reveals the bubble chamber's capability of measuring the high momentum tracks that come from the Quadrupole-Triplet focussing system. The deployment of the multiwire proportional chambers (MWPC) of the EMI and the efficiency of the two-plane EMI is discussed in Section III. The "1/3-scale" IPF is described in Section IV, and the summary is given in Section V.

II. 15-FOOT BUBBLE CHAMBER MOMENTUM (CURVATURE, $K \doteq p^{-1}$) ACCURACY.

The curvature spectrum of the measured leaving tracks of the Quad-Triplet beam is shown in Fig. 1. The solid curves are the resolution functions ($\Delta K = 3.0/\ell(m)^2$ TeV^{-1}) that are independent of curvature for one-meter and two-meter long tracks. For example, a one-meter long 330 GeV muon has a 100% error in its curvature. It is clear that at these high momenta the bubble chamber accuracy is being pushed to its limit. In order not to bias the neutrino energy measurement and other kinematic variables, adequate track length (ℓ>1 meter) must be provided. For experimenters planning for work with the 15-foot bubble chamber at the Fermilab Tevatron Neutrino Facility, this factor must be carefully considered. Perhaps the EMI can be used to improve upon the intrinsic measurement accuracy of the bubble chamber.

III. THE EMI AS CONFIGURED FOR E-546

III.1. Geometrical Efficiency

Fourteen new MWPC's with improved multitrack resolution were developed and built by the Hawaii-LBL group.[2] These were added to the 25 existing ones[3] and were configured into two planes as shown (roughly to scale) in Fig. 2 in order to provide maximum geometrical efficiency to neutrino-induced dimuon events for which the negative muon was expected to be considerably more energetic than the positive one. Not shown in this figure is the hadron absorbing material that exists in front of the first plane (3 to 5 absoption lengths) and between the first and second planes (5.5 absorption lengths). The geometrical efficiency for this arrangement for the $\mu^-(\mu^+)$ with $p > 4$GeV/c from CC(CC) events of E-546 is $0.85 \pm .03$ $(0.91 \pm .03)$.

III.2. Muon Identification Efficiency

III.2.1. Electronic efficiency from "beam tracks".

The muons from neutrino interactions in the last part of the earth berm that pass through the bubble chamber, not only serve to more accurately locate the MWPC's relative to the bubble chamber track but serve to measure the electronic efficiency.[4] From a sample of 1586 tracks with momentum greater than 10 GeV/c that lie within 2.5 degrees in dip and azimuth to the neutrino beam centerline, eight are observed to interact. From this, one concludes that only 0.17% of these "beam tracks" are hadrons. The rest are muons.

By employing the standard techniques of using a track detected in the ith plane to ask whether it was detected in the jth plane, one can determine the electronic efficiency*, ϵ_i, of the ith plane (in the last two-thirds of the run),

$$\epsilon_1 = 94 \pm 1\%,$$

$$\epsilon_2 = 92 \pm 1\%.$$

Another form of electronic inefficiency occurs because the time-duration of the beam spill sometimes exceeds the width of the time-gate. By comparing the number of beam tracks registering in both planes with the number expected from the two-plane efficiency $\epsilon_{12} \approx \epsilon_1\epsilon_2$, one can deduce the fraction of the beam that falls outside the gate. During one segment of the run this was 0.05, while during another it was nearly zero.

Seventeen (15)% of the time multiple in-time encodings occur as the muon passes through the first (second) EMI plane. Most are due to δ rays or showers. Figures 3a,b show the number distribution of extra hits for planes 1 and 2. For example, 252 of the 1480 "beam tracks"(17%) produce more than one encoding in the first plane. Figures 4a,b show how far away the extra hits are from the predicted muon coordinates, while Figures 5a,b show the same thing for a selected subset of N=1 or 2 extra hits, which are 12% (13%) of the beam tracks for plane 1(2). The "crucifix" pattern of Figs. 4a,b is produced by false solutions of our MWPC reconstruction program

*This includes the MWPC software reconstruction efficiency for ≥1C solutions.

(EMIKE). The spurious solutions become excessive the larger the electromagnetic shower of δ rays becomes. δ rays are responsible for part of the horizontal arm of the crucifix. We consider this part of the in-time background.

III.2.2. Electronic efficiency from muons from neutrino interactions.

The one track from a neutrino interaction that has the hightest transverse momentum and has $p > 25$ GeV/c is very likely a muon. In a subset of the data sample (the Hawaii portion), these muons have been used to determine the electronic efficiency of the EM1 planes in a way similar to that used with beam tracks. The results,

$$\epsilon_1 = 0.92 \pm 0.01,$$

$$\epsilon_2 = 0.86 \pm 0.02,$$

show that the efficiency of this second plane was lower in this part of the data. The early part of the experiment had several inefficient MWPC's.

III.2.3. In-time background.

Figures 6a(b) shows the hit* pattern relative to the projected position of 1105 leaving hadron candidates** in the first (second) plane. Punch through is clearly evident in the first plane and is much less so in the second one. The local density, ρ, of in-time hits in the second plane as a function of the momentum of the projected track is:

*All "EMIKE" solutions with ≥1C
**p>4GeV/c

$$n_2 = 0.032 \text{ hits/m}^2 \ (N_{hits}<3), \quad 5<p< \ 10 \text{ GeV}$$
$$= 0.025 \text{ hits/m}^2 \ (N_{hits}<3), \ 10<p< \ 20 \text{ GeV}$$
$$= 0.078 \text{ hits/m}^2 \ (N_{hits}<3), \ 20<p< \ 100 \text{ GeV}$$

The typical coulomb scattering radius that contains 86% of muons at the second plane is, r (cm) = 100/p(GeV/c). Thus, the probability that such a circle would contain a background hit for a 5 GeV/c particle is $\pi \times (.2)^2 \times 3.2 \times 10^{-2} = 0.4\%$.

IV. THE INTERNAL PICKET FENCE (IPF)[5]

IV.1. Geometrical Efficiency

IV.1.1. E-546 arrangement as a 1/3-scale model.

A 1/3-scale IPF was placed inside the bubble chamber vacuum tank immediately downstream of the one-inch thick (stainless steel) 12-foot diameter spherical chamber body and upstream of the super conducting coil vacuum-cryostat as shown in Fig. 2. Particular care was taken to shield the pickets with super-insulation from the 27°K chamber body temperature. Furthermore, each picket was placed in a thin stainless steel pouch, filled with an Argon gas mixture at room temperature and atmospheric pressure. Each of the 16 pickets had an active area of 0.1m x 1.0m and was constructed electrically as though it were a drift chamber with all the sense wires ganged together. The sense wires (20 μm diameter) and field wires (75 μm diameter) alternated with 5.4 mm spacing. The field wires and the two parallel 0.1m x 1.0m planar cathodes (which were spaced 2 x 5.4 mm apart) were at ground

potential, whereas the sense wires were at positive potential (typically 1.5kV). During the latter two-thirds of E-546, the gas mixture was Ethane(50%)-Argon(50%). Prior to that it was Argon(80%)-CO_2(20%), the same as the MWPC gas. A more detailed view of the picket arrangement is shown in Fig. 7. The units were placed vertically on the surface of a 2.0 meter radius cylinder. They spanned the bubble chamber coordinates from y = -110 cm to y = 110 cm* and in x as shown in Fig. 7. Thus the geometrical efficiency was

$$\epsilon_{Geom} = \frac{16 \times 10 \times 100}{2(110) \times 2(122)} = 0.40$$

IV.1.2. New configuration and improvements.

The new pickets will be twice as long, will be as close to each other as possible and will cover the area from y = -110 cm to y = 110 cm and z from -100 cm to 100 cm, giving nearly 100% geometrical efficiency. Each will contain an Fe^{55} source to monitor its gain, and will have a variable voltage placed on the field wires to allow for better electron collection.

IV.2. Electronic Efficiency

The inserted graph to the right of the pickets in Fig. 7 shows the value of the z-component of the magnetic field at the picket as a function of Z. There is a very large $\vec{E} \times \vec{B}$ effect on the drifting electrons that seriously delays, and possibly prevents, the formation of the electron avalanche on

*x is in the neutrino beam direction.

the sense wire. Fig. 8 is the time difference, Δt, between the IPF and the EMI "prompt signals". The time unit is $(28\text{MHz})^{-1}$ = 35.7 nsec, the period of the master clock. Delays of 0.5 μsec are not uncommon. In what follows, an in-time picket is one which has a value of Δt from 0 to 20 clock counts.

The electronic efficiency of the IPF is determined by using the beam tracks that exit the bubble chamber in the region of the IPF and match in both EMI planes. From rolls 1588 and 1615 there were 493 such beam tracks that had in-time matches in both planes. Of these, 87 had an in-time IPF hit, 5 of which had more than one picket "firing". Eighty of the 87 had an in-time hit in the picket nearest to the muon path. The exact picket locations were not yet known.

If one further requires that a beam track (muon) at the IPF have a Z coordinate of -118 to -18 cm or 4 to 104 cm, and Y coordinate of -113 to 113 cm, one finds 79 in-time signals in the nearest picket from 311 muons: Thus

$$\begin{array}{l}\text{Average picket}\\ \text{electronic efficiency}\end{array} = \frac{79/311}{.33} = 0.77$$

In other words, if a muon passes through the 0.1m x 1m sensitive region of a picket, the probability of the picket giving a signal is 0.77.

IV.3. <u>IPF "Triggering" Efficiency</u>

IV.3.1. Charged current events of E-546.

In a sample of 698 events which have an identified $\mu^{\pm}$ in both EMI planes and have $|Z_{vtx}|<110$ cm, 461 have an in-time

signal in the IPF. Thus the "triggering efficiency" of the IPF for CC events of E-546 is

$$\epsilon_{CC} = 461/698 = 0.66.$$

This efficiency shows little or no dependence on any of the following:

a) distance of the event vertex from the IPF,

b) momentum of the [illegible],

c) charged multiplicity.

The average number of pickets giving an in-time signal is 1080/698 = 1.55. If the number of pickets reporting were Poisson distributed, one would calculate the inefficiency to be $e^{-(\bar{n} = 1.55)} = 0.21$. That this number is different from 1-.66 = .34 is evidence that one does not have a Poisson distribution. The average number of pickets firing on those events that have at least one picket reporting is 1080/461 = 2.34.

IPF Background: If one looks in a random 20-clock count interval somewhere in the range 160 to -60 or 60 to 160, one finds 22 signals. This result shows there is a 22/698=0.03 accidental rate.

IV.3.2. Dimuon events of E-546 ("GSCAN" candidates).

The IPF was used to prescan for dimuon candidates by forming a ≥5-fold time coincidence with 1 or more pickets and 2 or more hits in the first EMI plane and 2 or more hits in the second EMI plane. The off-line diagnostic program (called

"GSCAN") that was used to "scan" the EMI tapes immediately after the completion of each roll of bubble chamber film to ascertain that all equipment was working properly, was able to form the above ≥5-fold coincidence, and to provide the roll/frame number and the upstream view of the IPF and EMI "hit pattern" of dimuon candidates. Fig. 9 is a typical GSCAN candidate computer print-out. Within 1/2 hour of taking the last picture of experiment E-546, all the magnetic tapes had been processed and the dimuon candidates (called GSCAN candidates) recognized. In general there were ≈ 50 GSCAN candidates per 1500 picture roll of film, of which 10 of the GSCAN candidate frames actually had an event in the picture. (There were about 180 interactions per roll.) If we had so chosen, we could have given first priority to measuring the leaving tracks of those 10 events on each roll. Because the IPF was working properly only for the last two-thirds of the experiment (after roll 1487) we decided not to use this method but measured the leaving tracks of all events. Had we chosen to use the GSCAN approach we would have found 37 of the 56, or 0.66 ± .11, of the dimuon events in this latter portion of the experiment. This method would have found dimuons ten times faster than measuring all leaving tracks. With a full scale IPF we would have found about 90% of them. GSCAN would have lost dimuon events where the two muons struck fewer than two MWPC's in either EMI plane. This is expected to happen about 10% of the time. Events shown in Figs. 10.2,

10.10, and 10.11 are examples of this type if the extra MWPC had not had an extra in-time hit in it. Figs. 10.1-10.12 show isometric hit patterns for all the dimuon candidates found by GSCAN in the Berkeley data sample. It missed only three, those shown in Figs. 10.13-10.15.

In the Berkeley-Hawaii sample of 23 dimuons found by GSCAN, there were 68 in-time pickets reporting, giving: 68/23 = 2.70 ± .34 pickets per GSCAN candidate, which is one standard deviation higher than the corresponding number for normal CC events of 2.34. With an IPF with improved geometrical and electronic efficiency any energy dependent bias on triggering efficiency will be negligible.

IV.3.3. Neutral current (NC) events of E-546.

One can use the leaving track measurements of CC events to estimate how well the IPF and the 2-plane EMI, configured as it is for E-546, would perform in a NC experiment. First, one must estimate what the IPF triggering efficiency would be if one were to remove the muon from the CC events that caused, on the average, 1.55 pickets to report and had a 0.66 probability of firing at least one picket. The probability that the muon would fire one picket = 0.30 x 0.77 = .23. Thus one would expect the average number of pickets for a NC

event to be $\approx 1.55 - .23 = 1.32$. If we now scale down the NC Poisson factor ($1-e^{-1.32} = .73$), by the ratio of the observed CC IPF firing efficiency, 0.66, to the CC Poisson factor ($1-e^{-1.55} = .79$) one obtains,

$$\epsilon_{NC}^{IPF} = \frac{0.66}{0.79} \times 0.73 = 0.61,$$

as the estimated triggering efficiency of the IPF for a NC event of E-546.

The geometrical efficiency of the EMI for leaving hadrons of E-546 is determined from a sample of 1922 CC events (with 1623 μ^- and 299 μ^+). There were 663 positive leaving hadrons out of 728 with $p > 4$GeV/c that would have hit the EMI if they had been muons, and 330 out of 424 negatives that would have done the same thing. Thus the geometrical efficiencies for leaving hadrons are:

$$\epsilon^+ = 663/728 = 0.91$$

$$\epsilon^- = 330/424 = 0.78$$

If one restricts this analysis to only μ^- type events one obtains, $\epsilon^+ = 0.94$ and $\epsilon^- = 0.82$.

IV.3.4. Predicted performance for NC identification for dichromatic experiments E-380/388.

With the improved geometrical coverage and electronic efficiency, the triggering efficiency of the IPF for the NC events of E-380/388 should be nearly 1.

Because we have not made full energy measurements on

normal CC events yet, it is too early for us to predict what the geometrical efficiency of the EMI for hadrons of E-380/388 will be.

V. SUMMARY

V.1. The Curvature ($K \equiv p^{-1}$) Accuracy of the 15-Foot Bubble Chamber is, $\Delta K \approx 3/L^2(m)$ Tev^{-1}.

V.2. The Geometrical Efficiency of the 2-Plane EMI for CC ($\overline{CC}$) Events of E-546 is 0.85 ± .03 (0.91 ± .03).

V.3. The Electronic Efficiency of the 1st (2nd) Plane is .94 ± .01 (.92 ± .01).

V.4.1. The geometrical efficiency of the IPF for E-546 is 0.30. For the improved IPF it will be nearly 1.

V.4.2. The electronic efficiency of the average picket is 0.77.

V.4.3.1. The efficiency for the IPF to "fire" on an E-546 CC event is 0.66.

V.4.3.2. The efficiency for the IPF to "find" dimuon events from the EMI tapes is 0.66 ± .11.

V.4.3.3. The efficiency for the IPF to "fire" on an E-546 NC event is ≈ 0.61. The geometrical efficiency of the 2-plane EMI for positive (negative) hadrons with p>4GeV/c from CC events is 0.94 (0.82).

V.4.3.4. The efficiency for the improved IPF to "fire" on a NC event of E 380/388 will be nearly 1. It is too early for us to predict what the geometrical efficiency of the EMI will be for hadrons.

VI. ACKNOWLEDGMENTS

The Fermilab staff is to be commended for installing such a large test IPF system. It came very close to allowing us to get out our dimuon measurements ten times faster than previously. Special thanks goes to Taka Kondo who was responsible for rearranging the electronics and other hardware for the unproved 2-plane EMI. Dan Curtis provided many of the on-line software changes. M. Atac and J. Urish developed the IPF pickets. We are grateful to the LBL mechanical and electronic technicians for their work in constructing the new MWPC's and digitizers. Our thanks goes to the scanning and measuring personnel at all our institutions for the painstaking care they have given to these high energy neutrino events.

REFERENCES

1) Berkeley (Univ. of Calif. and LBL): H. C. Ballagh, H. H. Bingham, W. B. Fretter, T. Lawry, G. Lynch, J. Lys, J. P. Marriner, J. Orthel, M. D. Sokolov, M. L. Stevenson, G. P. Yost; Fermilab: B. Chrisman, D. Gee, A. Greene, G. Harigel, F. R. Huson, C. T. Murphy, E. Schmidt, W. Smart, J. Wolfson; Univ. of Hawaii: R. J. Cence, F. A. Harris, M. D. Jones, S. I. Parker, M. W. Peters, V. Z. Peterson, N. Wyatt; Univ. of Washington: T. H. Burnett, D. Holmgren, H. J. Lubatti, K. Moriyasu, H. Rudnicka, G. M. Swider, E. Wolin, B. S. Yuldashev; Univ. of Wisconsin: J. R. Benada, U. Camerini, W. Fry, R. J. Loveless, P. McCabe, D. Minette, D. D. Reeder.

2) J. Orthel, S. I. Parker, D. Gee, et al (in preparation).

3) R. J. Cence, F. A. Harris, S. I. Parker, M. W. Peters, V. Z. Peterson, V. J. Stenger, G. Lynch, J. Marriner, F. T. Solmitz, and M. L. Stevenson, Nuclear Instruments and Methods 138, 245 (1976).

4) J. Marriner, "E-546 MWPC Efficiency", LBL Physics Note 851, 8 June 1978.

5) M. L. Stevenson, "The 'Internal Picket Fence': A Device That Could Reduce the Background in the Phase I External Muon Identifier", LBL Physics Note 809 (2 Oct. 1975); F. Harris, V. Z. Peterson, Univ. of Hawaii; and M. Atac, Fermilab; "Status of the Internal Picket Fence for the Fermilab 15-Foot Bubble Chamber", U. H. Internal Report 26-76 (23 July 1976); M. Atac, F. A. Harris, and S. I. Parker, "Some Test Results From an Internal Picket Fence Chamber for the Fermilab 15-Foot Bubble Chamber", Fermilab TM-688 (24 Sept. 1976); M. Atac, F. A. Harris, S. I. Parker, V. Z. Peterson, and J. Urish, "Drift Chamber Performance in High Magnetic Fields", Fermilab TM-776 (in preparation); J. Lys, et al, "A Neutrino Bubble Chamber Experiment Using a 2-Plane EMI and an Internal Picket Fence", Bull. Am. Phys. Soc. 23, No. 4, 560 (1978).

FIGURE CAPTIONS

Fig. 1. The curvature distribution of the leaving tracks in experiment E-546. The resolution function, $\Delta K \approx 3/\ell(m)^2$ TeV^{-1} is shown for ℓ = 1m and ℓ = 2m long tracks.

Fig. 2. The geometrical arrangement of the EMI and IPF for experiment E-546. Not shown are the absorbing materials placed in front of the first and second EMI planes.

Fig. 3a(b). The frequency distribution of extra hits produced in the first (second) EMI plane by a pure sample of muons ("beam tracks").

Fig. 4a(b). The hit patterns of the extra hits relative to the predicted muon hit in the first (second) EMI plane for a pure sample of muons.

Fig. 5a(b). The same patterns except for low multiplicity hits, N extra = 1, 2.

Fig. 6a(b). The in-time background or punch-through of hadrons in the first (second) EMI plane.

Fig. 7. A "Neutrino interaction-eye-view" of the IPF arrangement for E-546.

Fig. 8. The IPF-EMI time difference, $T=t_{IPF}-(t_{1EMI}+t_{2EMI})/2$ distribution.

Fig. 9. A typical hit pattern and time and MWPC number summary for dimuon candidates found by the off-line diagnostic program GSCAN.

FIGURE CAPTIONS (continued)

Fig. 10.1-10.12. Isometric views of the hit patterns for the dimuon found by GSCAN in the Berkeley data sample.

Fig. 10.13-10.15. Isometric views of the hit patterns for those dimuon events of the Berkeley sample not found by GSCAN.

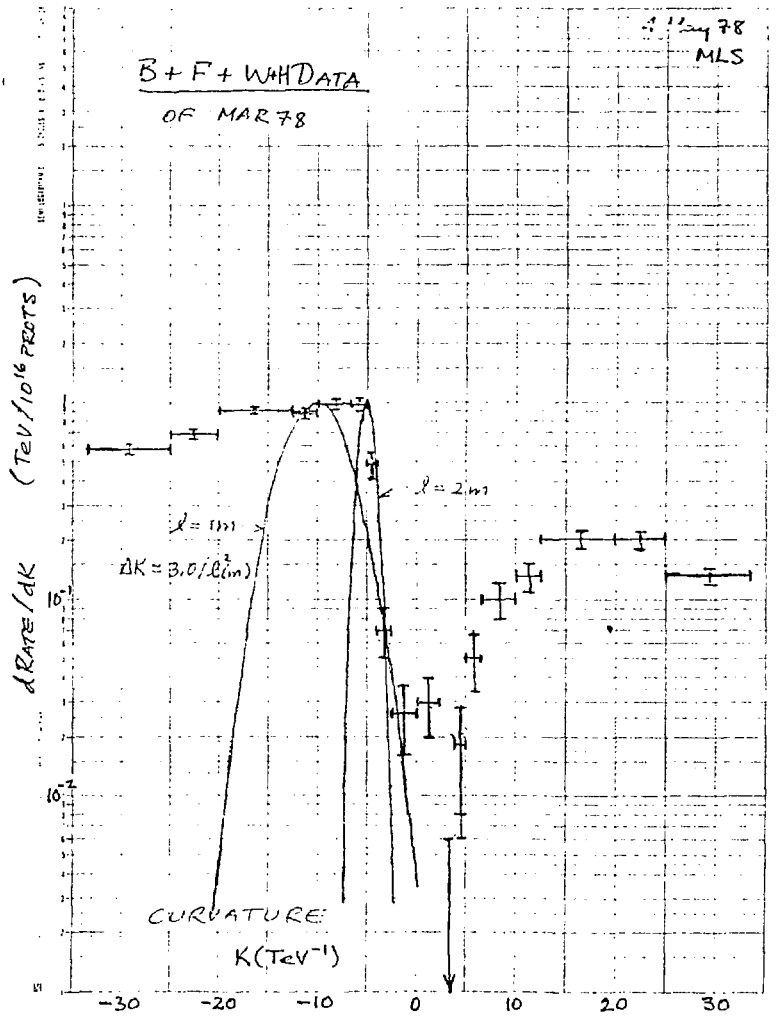
B + F + WHDATA
OF MAR 78
MLS
dRATE/dK (TeV/10^16 PROTS)
ℓ = 2m
ℓ = 1m
ΔK = 3.0/ℓ²(m)
CURVATURE
K(TeV⁻¹)
-30
-20
-10
0
10
20
30

Fig 1

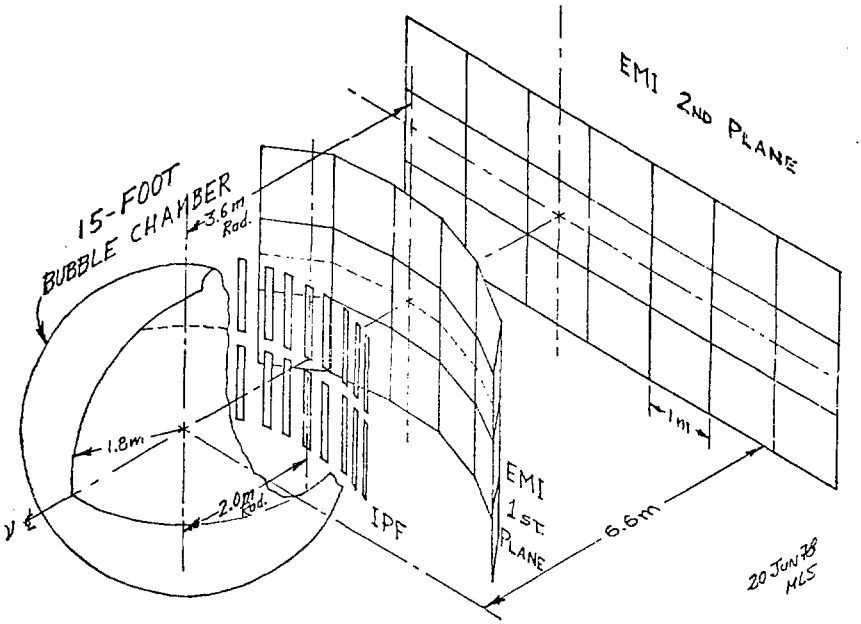
15-FOOT
BUBBLE CHAMBER
3.6m Rad.
1.8m
2.0m Rad.
ν
IPF
EMI 1ST PLANE
EMI 2ND PLANE
1m
6.6m
20 JUN 78
MLS

Fig 2

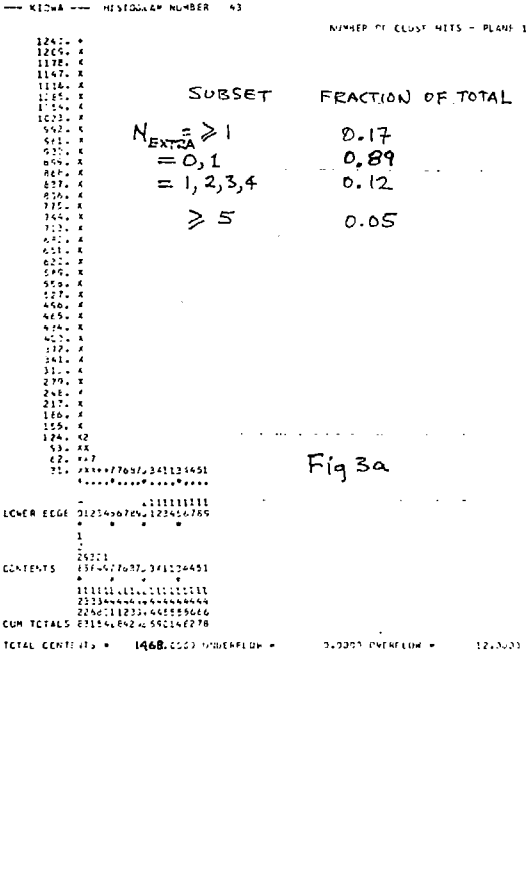

SUBSET	FRACTION OF TOTAL
$N_{EXTRA} \geq 1$	0.17
$= 0, 1$	0.89
$= 1, 2, 3, 4$	0.12
≥ 5	0.05

Fig 3a

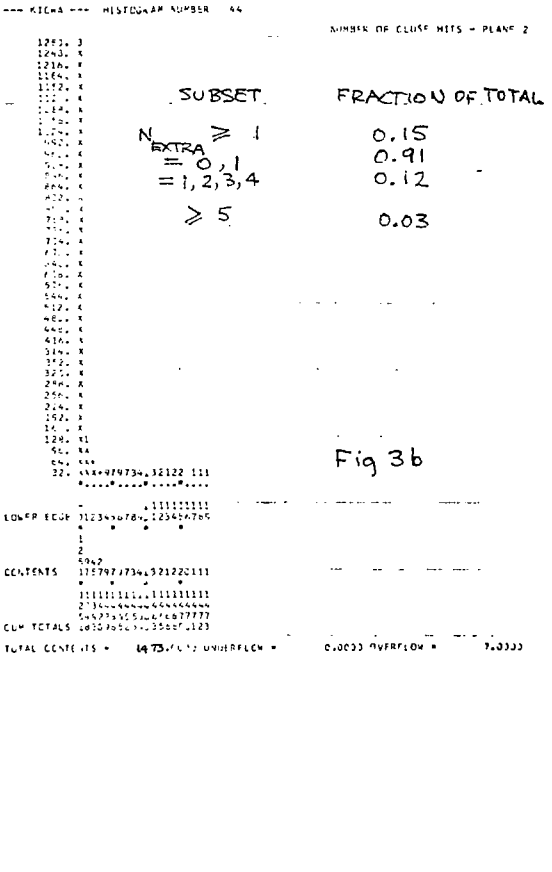

SUBSET	FRACTION OF TOTAL
$N_{EXTRA} \geq 1$	0.15
$= 0, 1$	0.91
$= 1, 2, 3, 4$	0.12
≥ 5	0.03

Fig 3b

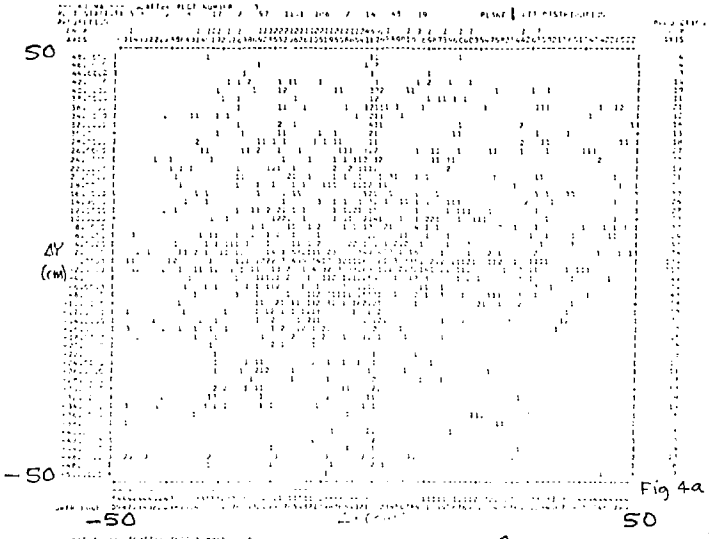

Fig 4a

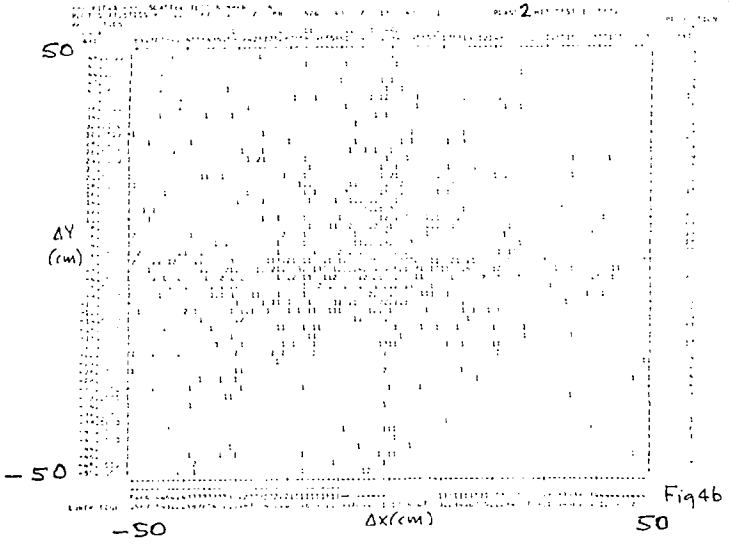

Fig4b

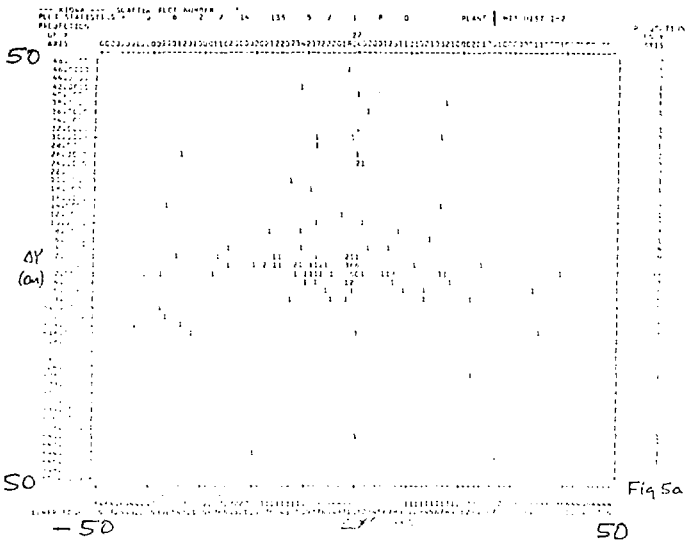

Fig 5a

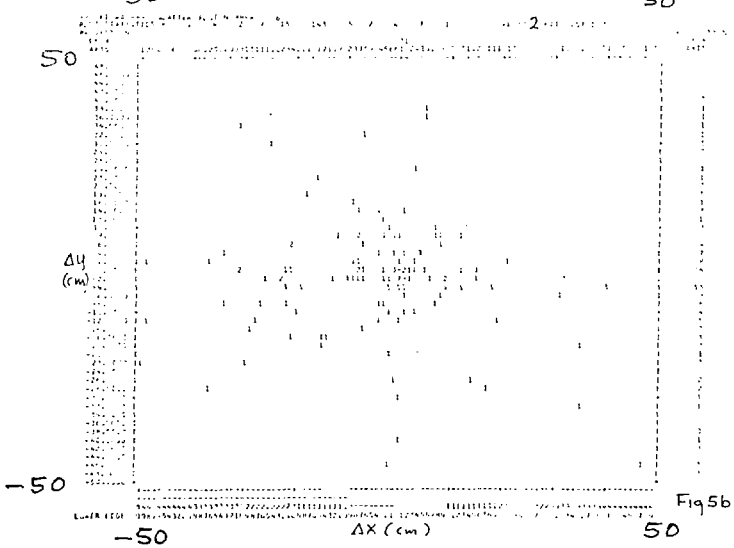

Fig 5b

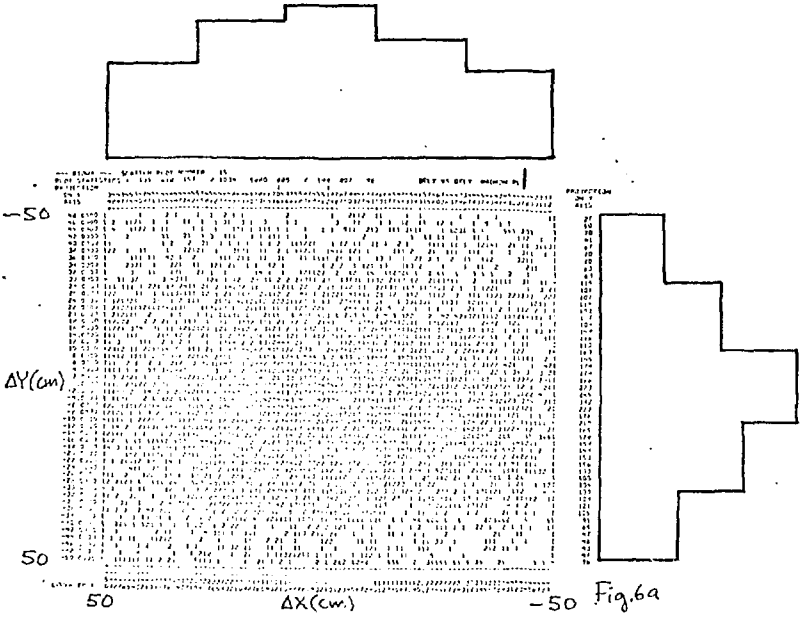

Fig.6a

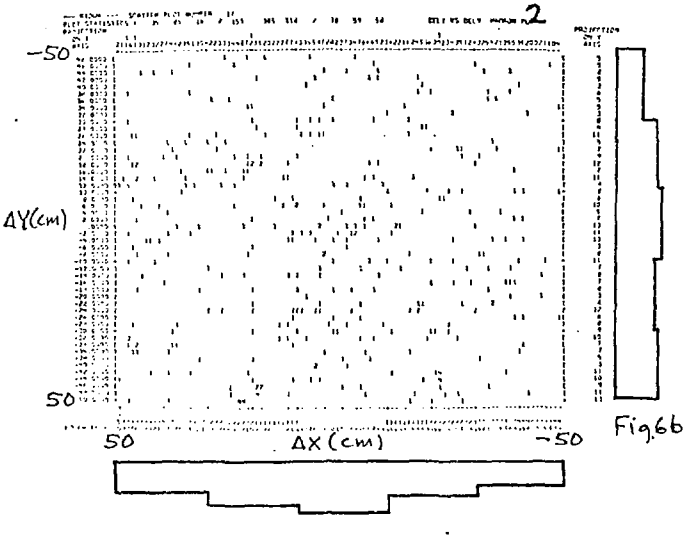

Fig.6b

3.

Location and geometrical efficiency of expt. 546

IPF chambers :

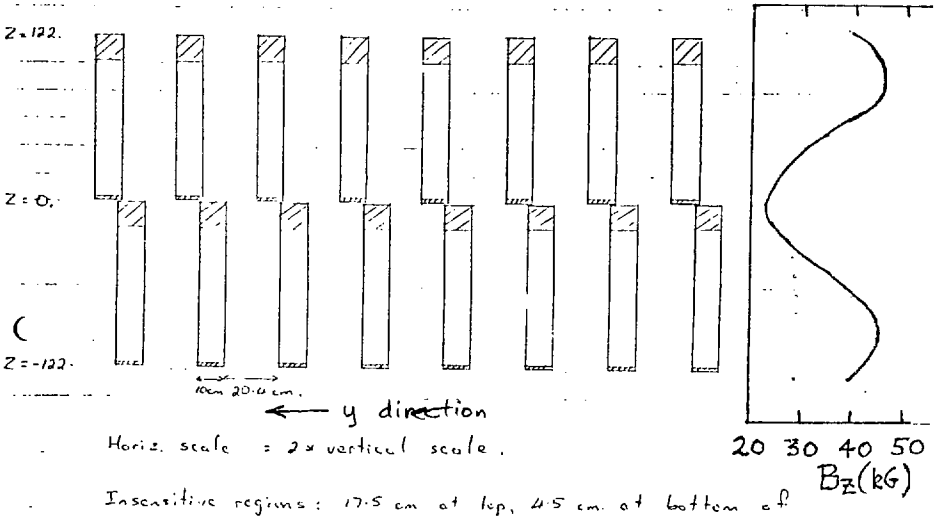

Horiz. scale = 2 × vertical scale.

Insensitive regions: 17.5 cm at top, 4.5 cm. at bottom of each chamber.

Chambers are on the surface of a cylinder with vertical axis and with radius 200 cm.

In b.c. coor. system, the chambers extend from $Y \approx -110.$ to $Y \approx +110.$

Geometrical efficiency $\approx \frac{16 \times 10 \times 100}{320 \times 244} = .30.$

Fig 7

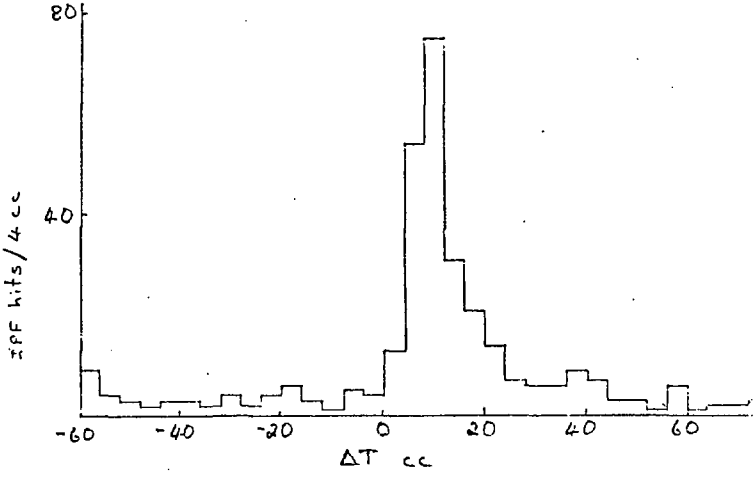

Fig. 8

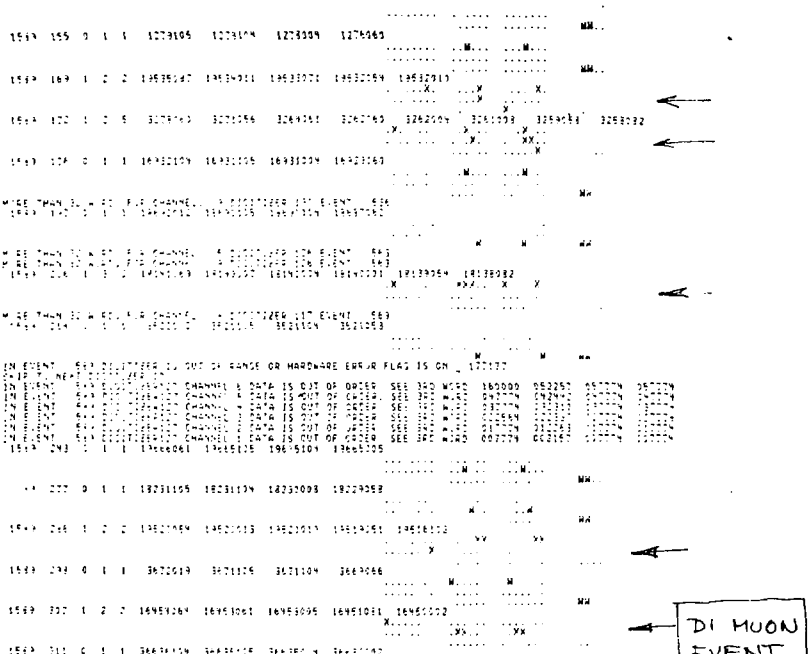

Fig 9

1500/818 (B)

96 9 61
95 12 53
94 5 56
10

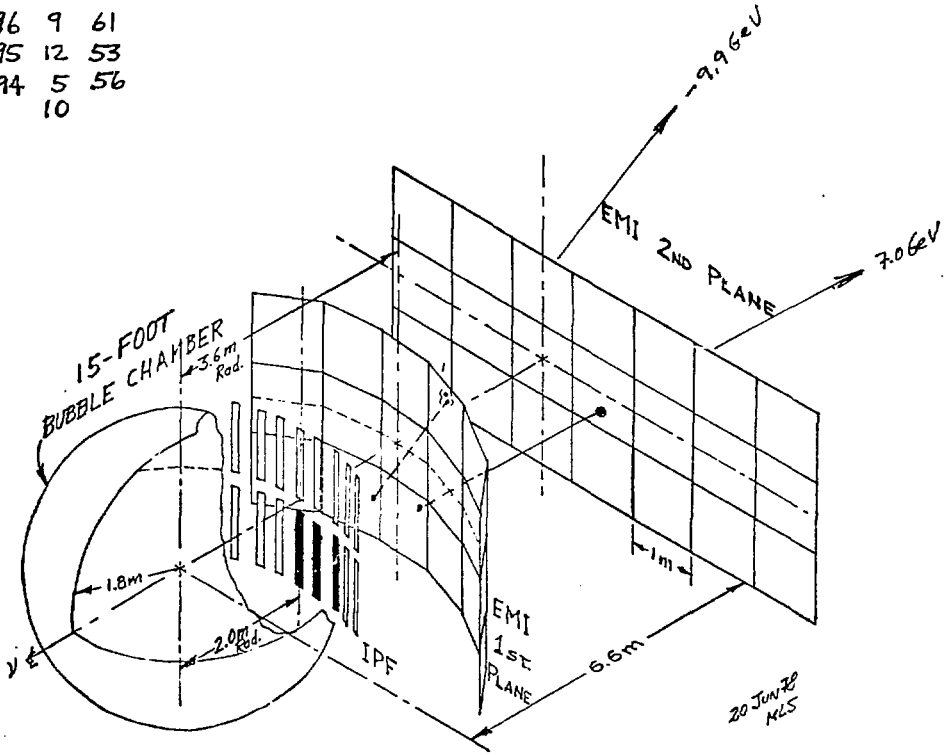

Fig 10.1

1526/918 (B)

101	9	56
95	15	53
102		52
97		

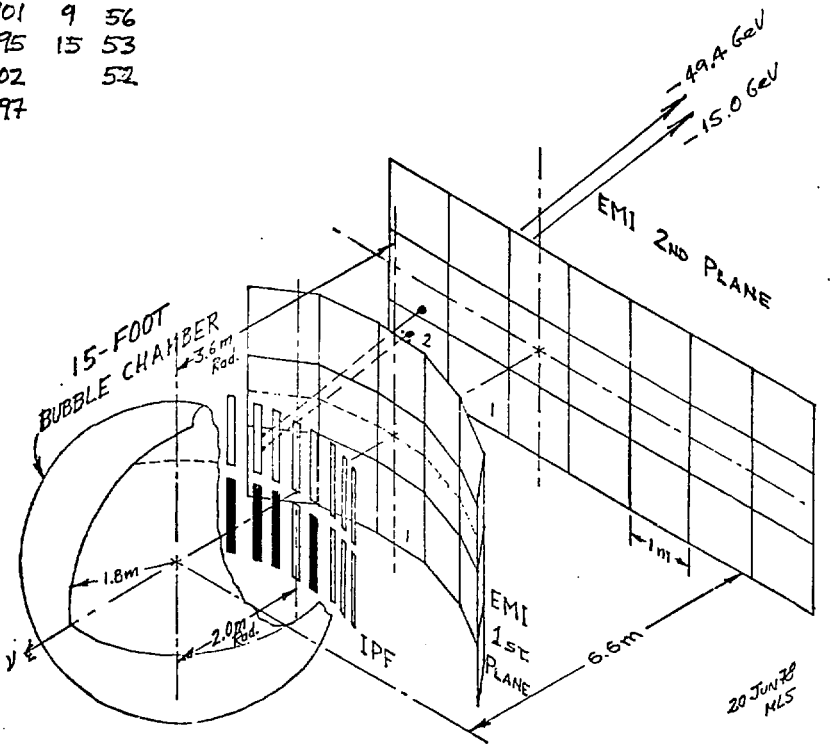

Fig 10.2

1526/1166 (B)

86 11 58
8 56

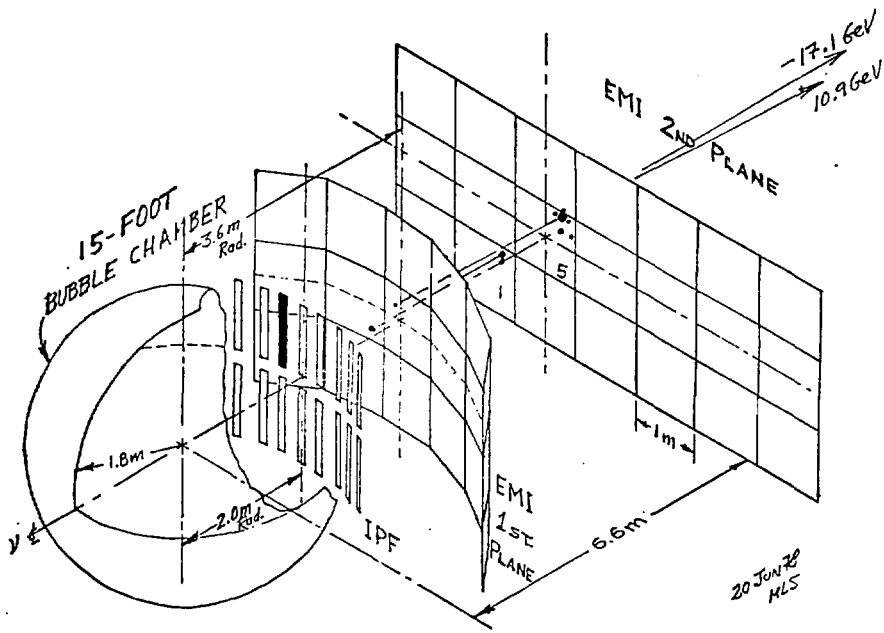

Fig 10.3

1589/307 (B)

81 5 64
2 61

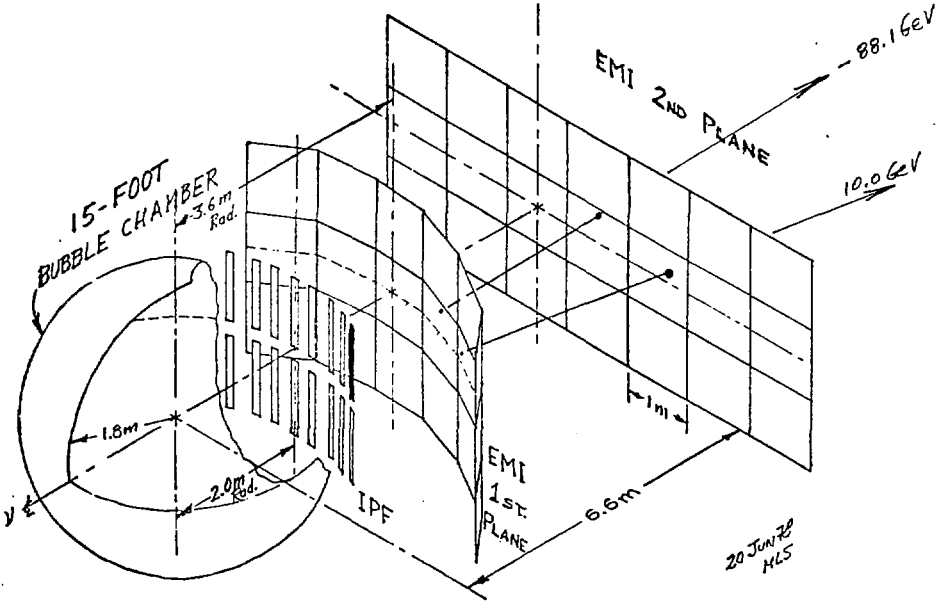

Fig 10.4

1589/1378 (B)

97 12 56
101 9 58
8

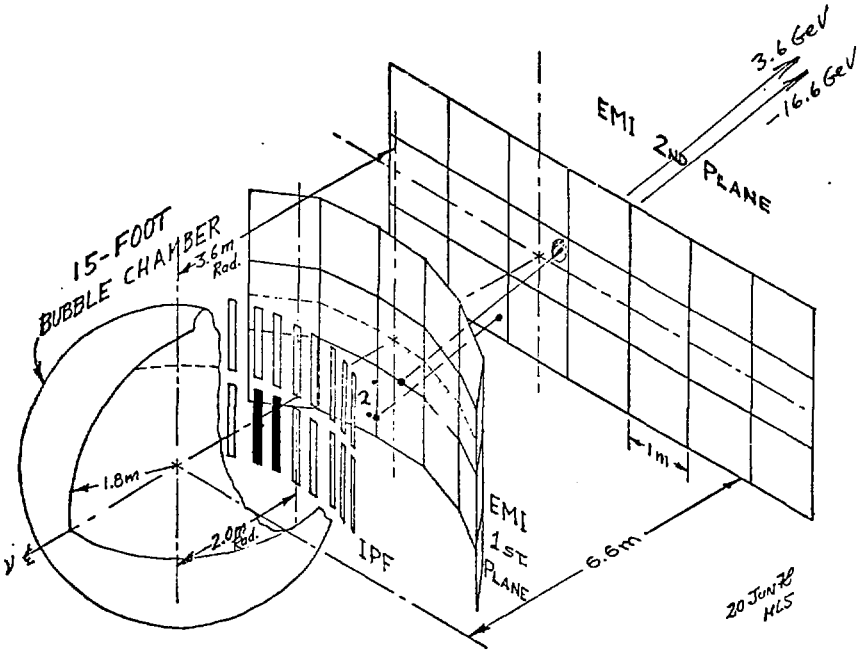

Fig 10.5

1605/1203 (B)

84 7 60
84 4 57

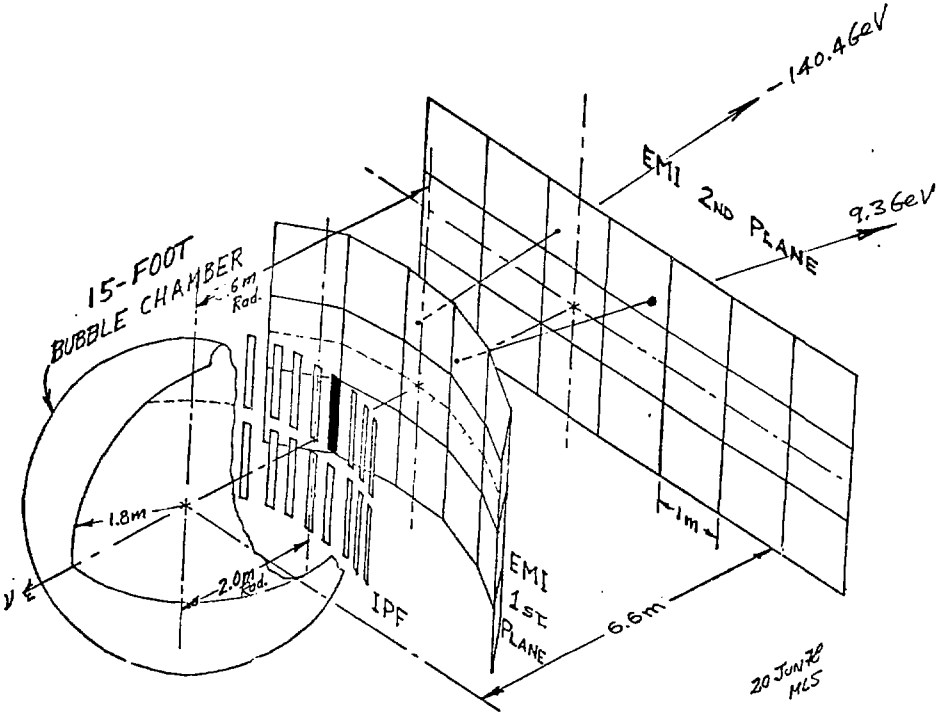

Fig 10.6

R/F = 1606/1451 (B)

4	2	2
97	11	67
95	5	52
93		
87		

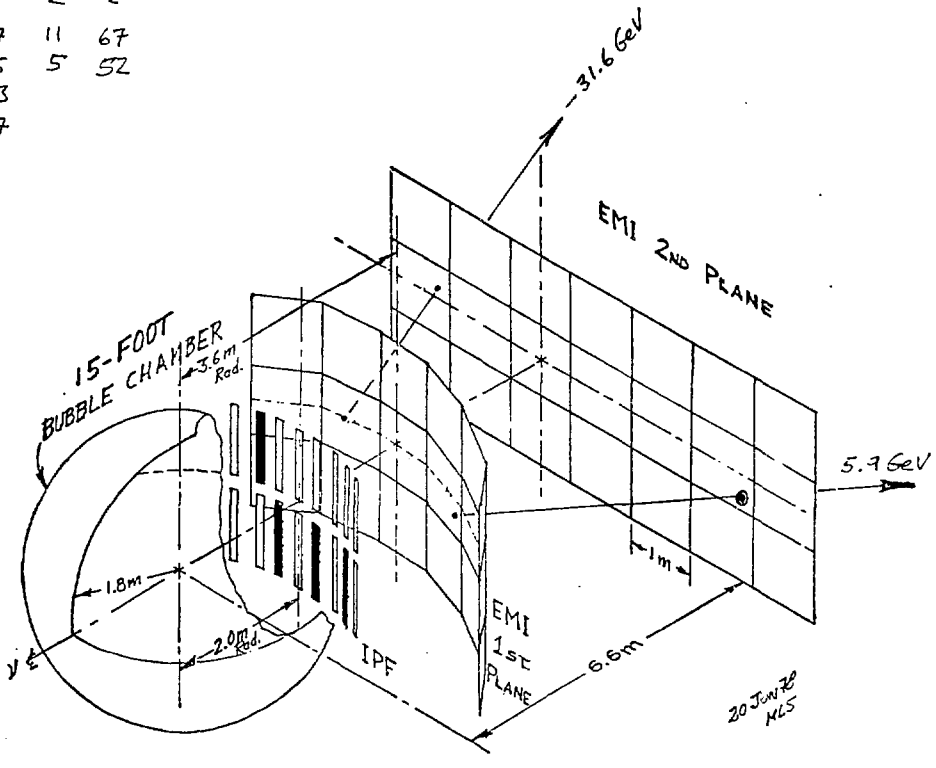

Fig 10.7

R/F = 1615/1918 (B)

82 8 55
84 2 67
83 5
81

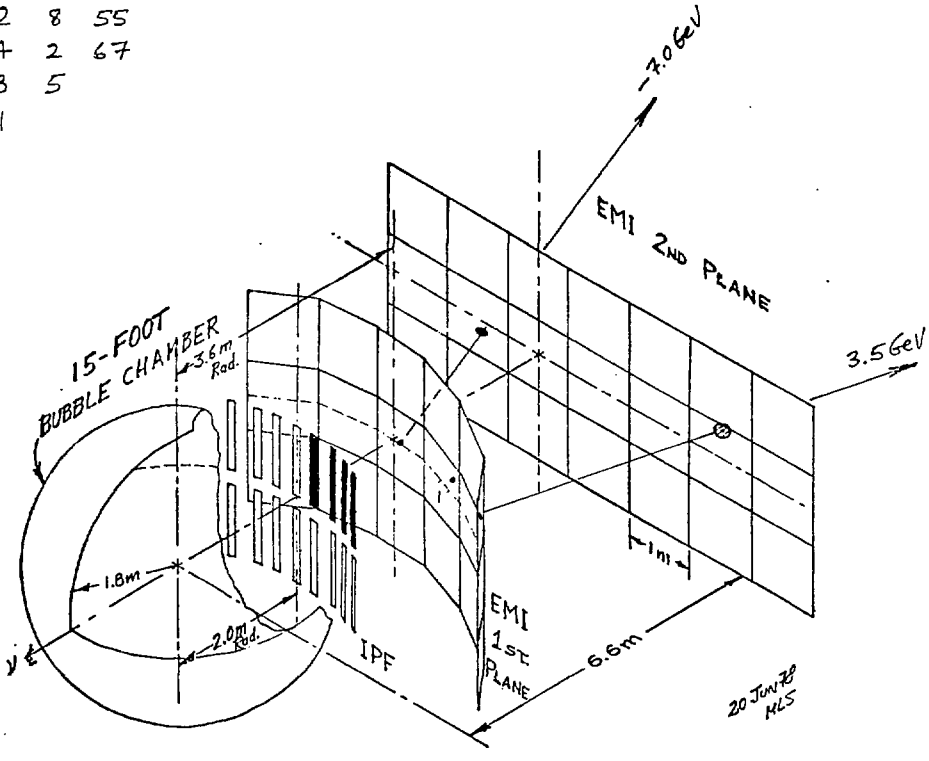

Fig 10.8

1656/565 (B)

84 11 55
85 10 54
82 8
86
87

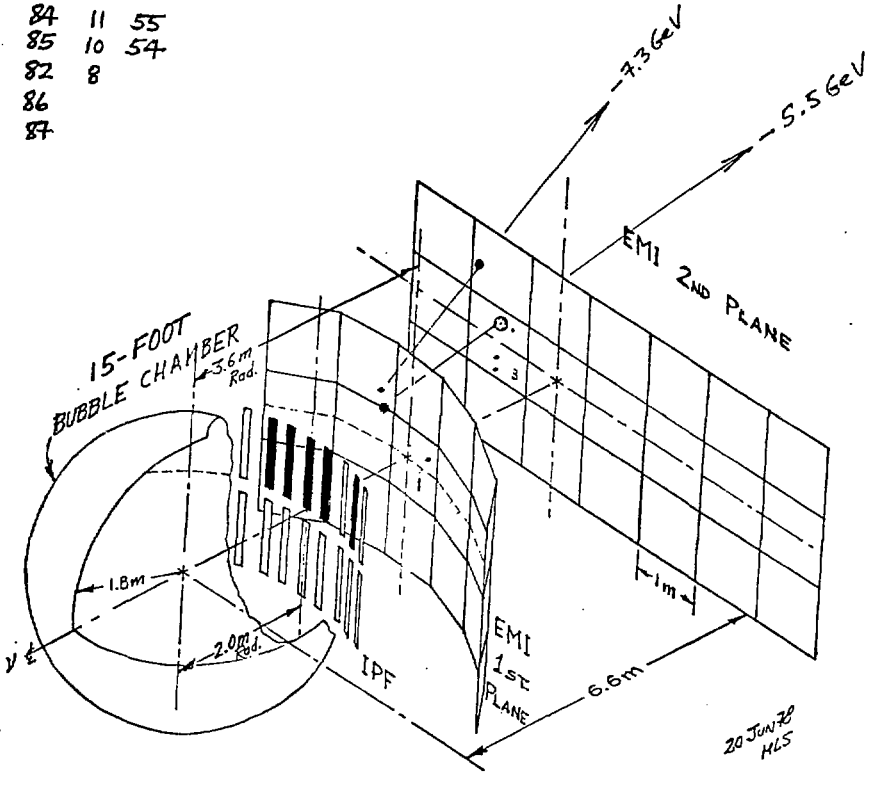

Fig 10.9

1518/746 (B)

-15 GeV has low C.L. in table 8

83	7	52
85	4	55
81	8	53

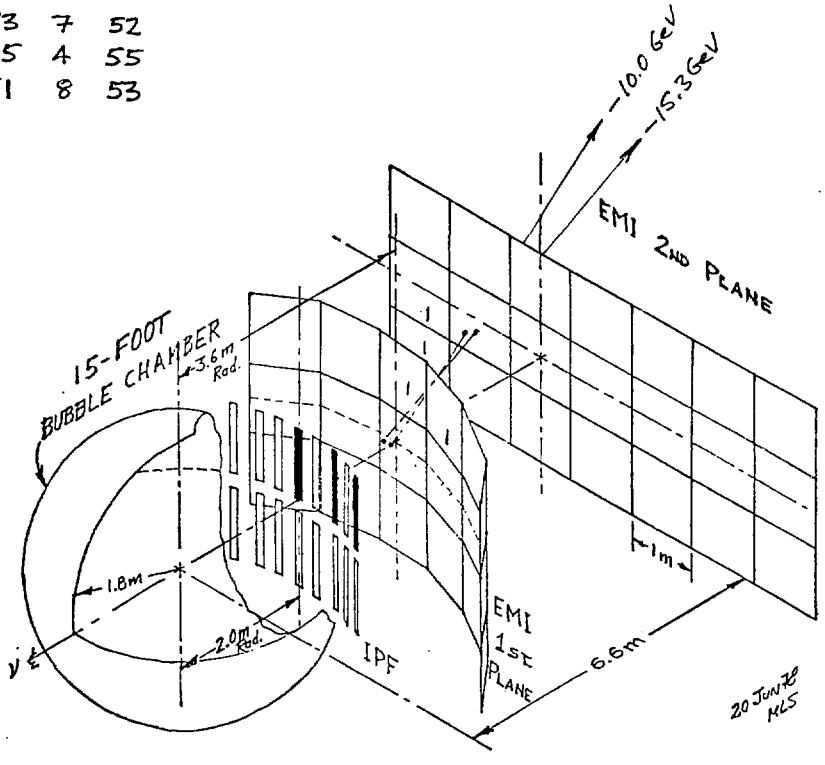

Fig 10.10

1627/977 (B) low CL's

99? 12 55
86 11 52

$\ell \approx 55$ cm.

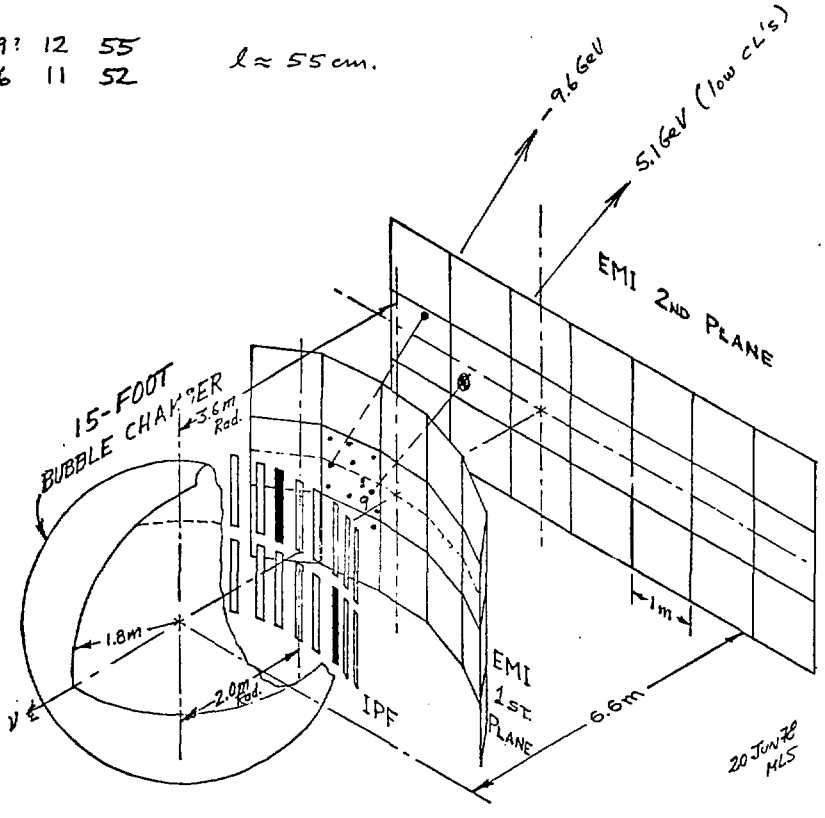

Fig 10.11

1627/2472 (B)

94 9 61
95 8 58
5 57
6
11
7

$\ell \approx 55$ cm

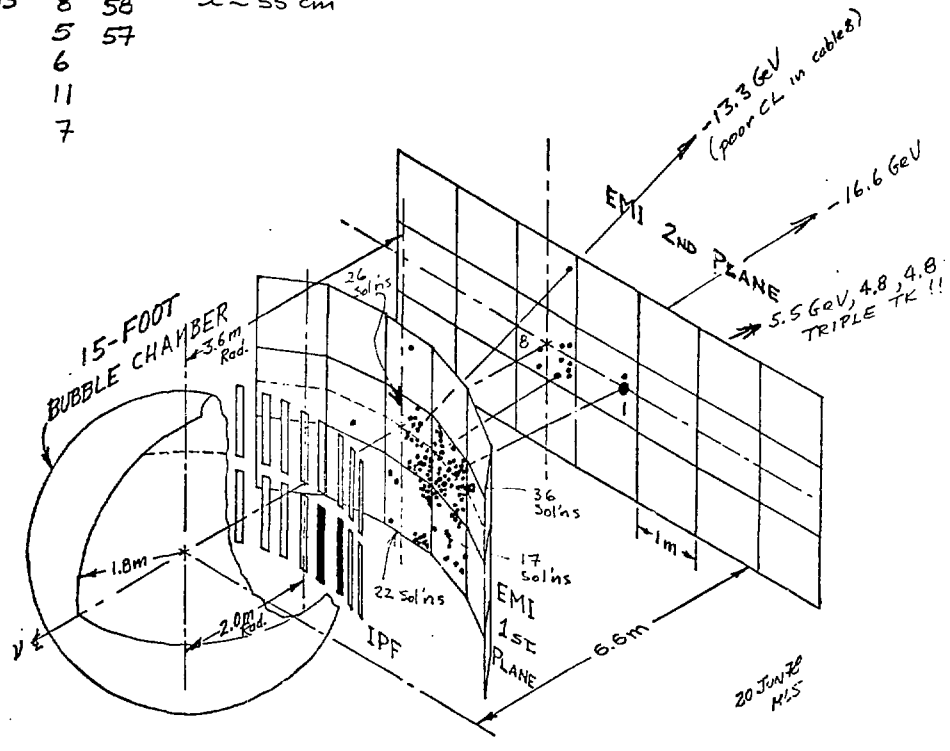

Fig 10.12

1580/1497 (B) NOT FOUND BY GSCAN

0 7 57
8
11
10

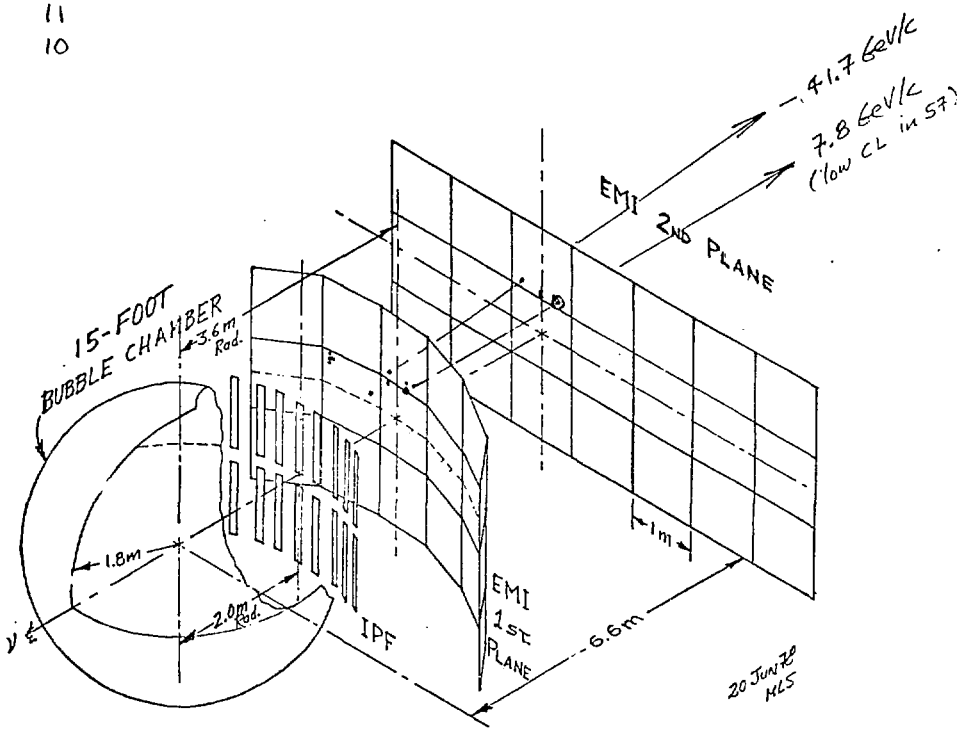

Fig 10.13

1531 / 941 (B) NOT FOUND BY GSCAN

0 8 58
61

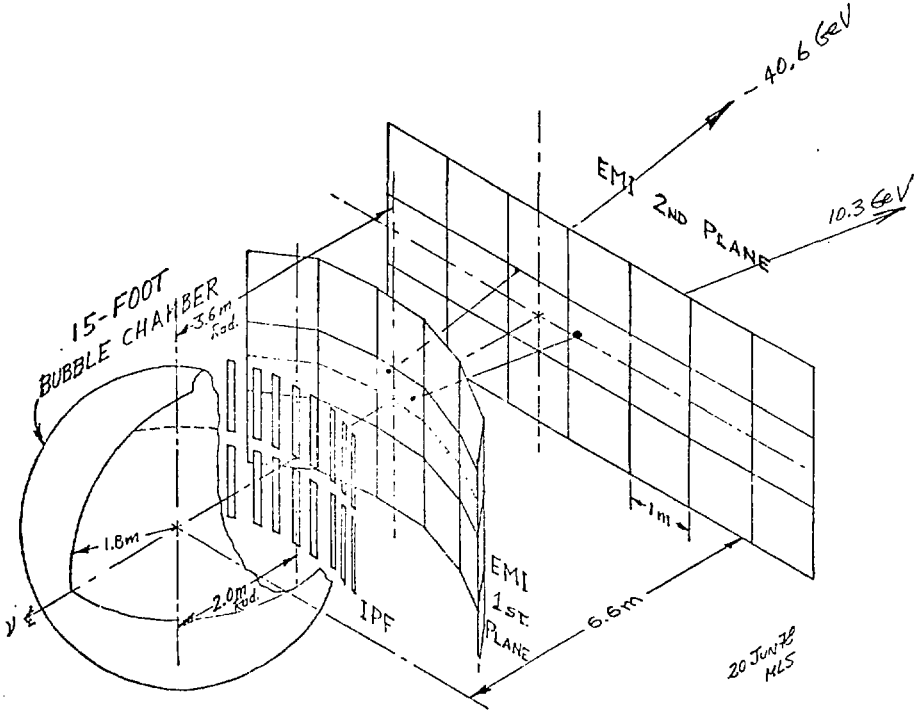

Fig 10.14

1526/1220 (B) NOT FOUND BY GSCAN

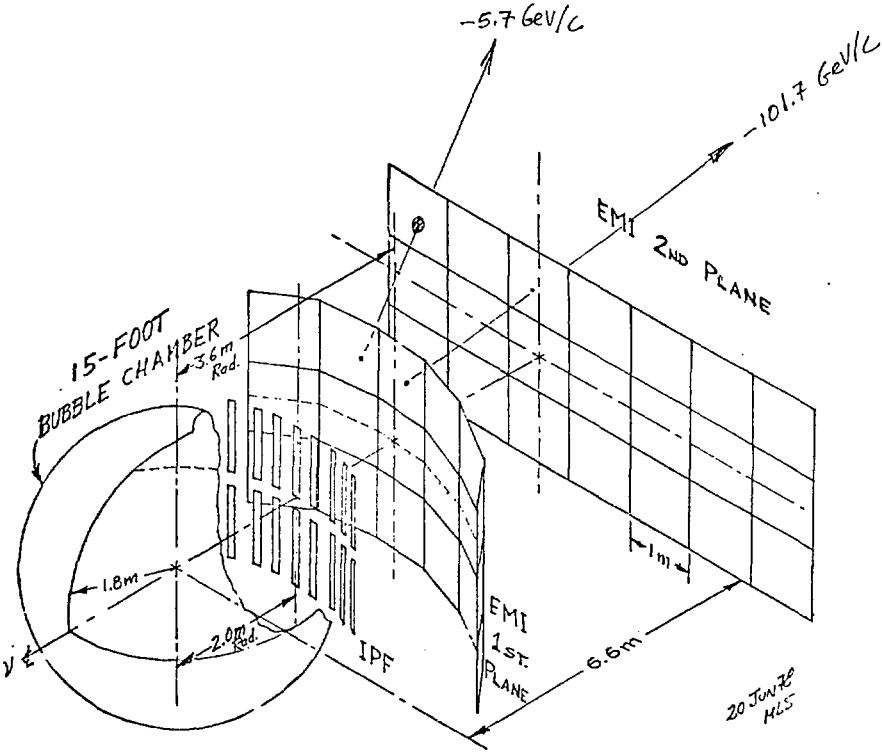

Fig 10.15